Journal of Nuclear Materials 390–391 (2009) 983–987

Contents lists available at ScienceDirect

Journal of Nuclear Materials

journal homepage: www.elsevier.com/locate/jnucmat

RF heated wall conditioning discharges in JT-60U

K. Itami *, N. Asakura, H. Tamai, S. Moriyama, A. Kaminaga

Japan Atomic Energy Agency, 801-1 Mukouyama, Naka, Ibaraki 311-0193, Japan

ARTICLE INFO

PACS:
52.25.Jm
52.40.Hf
52.50.Sw
52.55.Fa

ABSTRACT

In series of experiments in 2000 and 2008, helium wall conditioning discharges by ECRF heating (ECH) were extensively studied in JT-60U with $B_T = 3.6$ T and $P_{ECRF} \leqslant 2.5$ MW. Homogeneous ECH conditioning discharges were reproducibly obtained by applying the horizontal field as large as 0.2% of B_T. It was found that the horizontal field is effective to extend He plasma toward high field side from the fundamental resonant surfaces of ECH. The ECH wall conditioning discharge with $P_{ECRF} = 2.5$ MW and $t_{pulse} = 1.5$ s was applied after the plasma disruption with $W = 3.3$ MJ and the successful recovery of the current ramp-up with 0.5 V/m of ohmic electric field was obtained.

1. Introduction

In order to reduce impurity influx to the core plasmas and to control particle recycling level, first wall conditioning by the hydrogen and helium discharges, such as glow discharge cleaning (GDC) and Taylor discharge cleaning (TDC) are widely used in fusion devices [1]. Here, TDC utilizes tokamak discharges with short pulse, low power but high repetition rate [1]. The typical plasmas for TDC have parameters of $I_p = 50$ kA, $B_T = 0.7$ T and $t_{pulse} = 20$ ms and those plasmas are repeated every 3–5 s in JT-60U. Here I_p, B_T and t_{pulse} are the plasma current, toroidal field and pulse length, respectively. For the control of the recycling level, TDC with helium gas (He TDC) is applied for 3–7 min between the experimental discharges in JT-60U.

However, GDC cannot be utilized due to the stationary toroidal field in superconducting tokamaks, such as ITER and DEMO. There is also restriction on the applicable voltage on the superconducting poloidal coils and the toroidal electric field must be below 0.3 V/m. TDC plasmas would not break down in such low electric field conditions.

In order to address these issues, wall conditioning techniques using ion cyclotron range of frequency (ICRF) heating have been investigated in high toroidal field (B_T) conditions in TEXTOR [2], TORE SUPRA [3] and EAST [4]. There have been no study about wall conditioning using electron cyclotron range of frequency (ECRF) heating in B_T conditions in tokamaks, while few studies using RF heating by electron cyclotron resonance had been carried out in low B_T (~0.05 T) [5,6].

This paper presents particle recycling controls by helium conditioning discharges using ECRF heating (ECH) in high B_T conditions in JT-60U.

2. Experimental results

2.1. Production of ECH wall conditioning plasmas

In experimental campaign to investigate RF heated wall conditioning discharges in 2000, a few trials of wall conditioning discharges using ICRF heating and lower hybrid range of frequency (LHRF) heating with reduced toroidal field ($B_T = 0.73$ T) and a series of wall conditioning discharges using ECRF heating system[7] with high B_T ($B_T = 3.65$ T) were carried out.

ECRF heating (ECH) wall conditioning plasmas have been produced in the same experimental sequence with the tokamak discharges in JT-60U. The working gas of helium (He) was injected to the vacuum vessel of JT-60U in a pulsed gas puff just before ECRF heating. Coil current to produce poloidal field was not energized except for horizontal field coil current (I_H). The toroidal field strength $B_T = 3.65$ T is defined at the position of $R = 3.32$ m in JT-60U. $B_T = 3.65$ T and $I_H = 10$ kA were fixed in a series of discharges. Here R is the major radius of torus. Horizontal field strength with $I_H = 10$ kA is 0.5% of the toroidal field at the position of $R = 3.32$.

Visible video images from CCD camera were used as a tool to monitor the production of the plasmas by ECH, uniformity of the plasma and plasma wall interaction. In a series of discharge, shown in Fig. 1, ECRF power into the torus was $P_{ECRF} = 0.6$ MW. A typical ECH wall conditioning plasma (shot number E038071) is shown in Fig. 1(a) and (b). Amount of He gas puff was $Q = 2.4$ Pa m^3. In the first frame of visible video image, He plasma was initiated at the resonant position of the fundamental ECH, as shown in Fig. 1(a). Immediately after the initiation within 33 ms, the He

* Corresponding author.
E-mail address: itami.kiyoshi@jaea.go.jp (K. Itami).

0022-3115/$ - see front matter © 2009 Elsevier B.V. All rights reserved.
doi:10.1016/j.jnucmat.2009.01.254

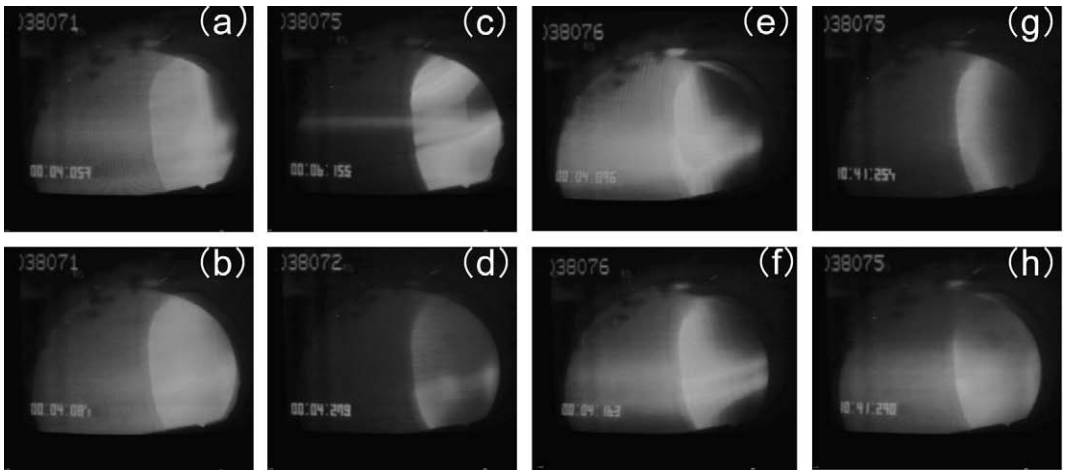

Fig. 1. Plasma images from CCD camera viewing inside the vacuum vessel. Lower part of the plasmas was hidden by structure in the viewing port. The center of torus is left. (a) Break-down with $Q = 2.4$ Pa m^3; (b) 33 ms later; (c) $Q = 2.4$ Pa m^3; (d) $Q = 7.5$ Pa m^3; (d) $Q = 0.8$ Pa m^3; (e) break-down with $B_T = 3$ T; (f) 33 ms later; (g) break-down of TDC and (h) the second and the last frame of TDC.

plasma expanded and filled the vacuum vessel, as shown in Fig. 1(b).

He gas amount was scanned in the range of $0.8\ \text{Pa m}^3 \leqslant Q \leqslant 12\ \text{Pa m}^3$. When Q is increased, the inhomogeneous stripes of He emission was seen in visible image, as shown in Fig. 1(c). When Q is reduced from the typical case, the brightness of He emission was homogeneously reduced, as shown in Fig. 1(d). In the discharge with $B_T = 3$ T, the resonant position of ECH was located at the inner wall. It was observed in the visible image that the plasma expanded from the resonant position mainly on the midplane, as shown in Fig. 1(d) and (e).

Effects of the ECH wall conditioning discharge can be measured by amount of hydrogen outgas. H_2 partial pressure and He partial pressure was measured with optical Penning gauge [8,9] located at bottom of the inner vertical port, U1 port. Details of gas measurement in JT-60U are shown in the Ref. [8]. In situ calibration of the optical Penning gauge had been done by cross-calibration with other gas gauges. As shown in Fig. 2, He neutral pressure was increasing during He gas injection from $t = 1$ s to $t = 4$ s. Then a ECH pulse with $P_{ECRF} = 0.6$ MW was injected from $t = 4$ s to $t = 5$ s. Due to the strong pumping effect of the ECH plasma, He pressure decreased rapidly from $t = 4$ s to $t = 5$ s. Increase in H_2

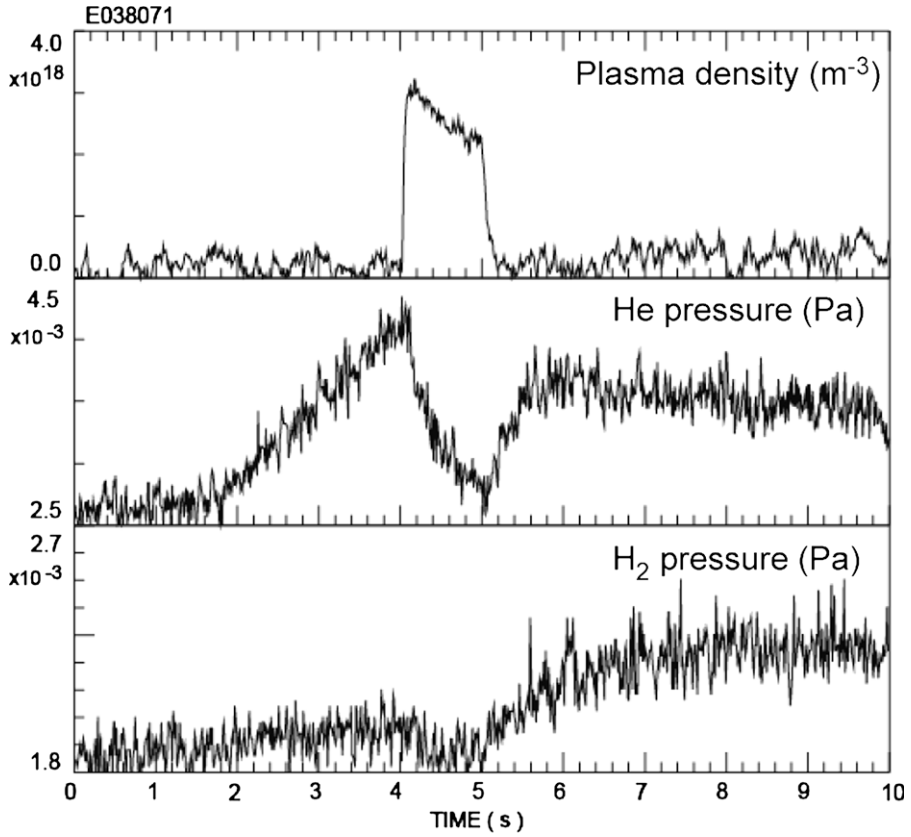

Fig. 2. Time evolution of the H_2 pressure and He pressure, measured by the optical Penning gauge at U1 port, during E038071.

pressure after $t = 5$ s is hydrogen outgas due to this conditioning discharge. The plasma density was averaged along the tangential chord of the CO_2 laser interferometer, whose length is 6 m.

It was also observed that H_2 pressure after He conditioning discharges was not increased while the plasma density was increased up to 1.2×10^{19} m^{-3} by increasing He gas filling with the same ECH power.

2.2. Comparison with He TDC

Effective amount of H_2 outgas was compared with the usual He TDC plasma after a disruption, caused by the plasma density limit. The visible images are shown in Fig. 1(g) and (h). Gate valves to cryogenic-pumps for the NBI system were closed during this comparison and the vacuum vessel was mainly pumped by the JT-60 vessel pumping system.

H_2 pressure was measured by the ionizing gauge in the residual gas analyzer (RGA) system, which was located at the end of the manifold of JT-60 vacuum pumping system. JT-60U is equipped with two vacuum manifolds and the total pumping speed is estimated to be $S = 8$ m^3/s.

Time evolution of the H_2 pressure (P_{H_2}) during the ECH conditioning plasma (with $P_{ECRF} = 1.27$ MW and $t_{pulse} = 1$ s) and TDC plasmas are shown in Fig. 3. Total amount of outgas is given by time integral of $P_{H_2}S$ for both conditioning discharges. 0.175 Pa m^3 of H_2 was pumped out within 1 min after the ECH conditioning discharge, while 1.55 Pa m^3 of H_2 was pumped out during TDC in 7 min and 0.22 Pa m^3 of H_2 in 1 min average of TDC. This result is extrapolated to the ECH wall conditioning discharges in the stationary B_T conditions. If the ECH pulse, with the same power ($P_{ECRF} = 1.27$ MW) and same pulse length ($t_{pulse} = 1$ s), is applied every 1 min, the H_2 outgas efficiency of ECH wall conditioning discharge is equivalent to 79% of that of TDC. In this extrapolation, the duty ratio of ECH power is 1/60. If the duty ratio is increased to more than 1/40 with the same ECH pulses, the efficiency of ECH conditioning discharge is estimated to be higher than He TDC.

2.3. Effect of horizontal field

Additional experiment in 2008 was carried out to investigate horizontal field effect and to produce the ECH wall conditioning plasmas with the second harmonic heating with $B_T = 1.86$ T. It was not possible to produce homogeneous plasmas without horizontal field both with fundamental and second harmonic ECH. On the visible video images, vertical band of He emission along the resonant surface of ECH was observed.

With both polarity of the horizontal field ($I_H = -4$ kA and 4–5 kA), ECH wall conditioning plasmas were successfully reproduced with fundamental ECH, as shown in Fig. 4(a). However, homogeneous ECH plasmas were not obtained and local He line emissions, as shown in Fig. 4(b), were observed with the second harmonic ECH, while $I_H = 3$–4 kA was applied.

The resonant surface of fundamental ECH for $B_T = 3.65$ T is located at $R = 3.08$ m and that of the second harmonic ECH for $B_T = 1.86$ T is located at $R = 3.14$ m. Both the major radii are positioned between the U1 chord for FIR laser interferometer at $R = 2.66$ m and the U2 chord for FIR laser interferometer at $R = 3.54$ m. Both the U1 and U2 chords are shown in Fig. 5. As shown in Fig. 6, the U1 plasma density is significantly smaller than the U2 plasma density when $I_H = 0$, indicating the ECH plasma did not expand toward the high field side for both the fundamental and the second harmonic ECH.

2.4. Recovery from the plasma disruption

The ECH wall conditioning discharge was applied after the deuterium plasma disruption in E048651 in 2008. Plasma parameters before the disruption was $I_p = 1$ MA, $B_T = 3.5$ T, $P_{NBI} = 19$ MW and the stored energy (W) = 3.3 MJ. After the He wall conditioning discharge (E048652) using the fundamental ECH with $P_{ECRF} = 2.5$ MW and $t_{pulse} = 1.5$ s, the next experimental plasma (E048653) successfully started up. Therefore, the recovery of the first wall condition after the plasma disruption was demonstrated by ECH wall conditioning discharge.

In Fig. 7, time traces of the discharge parameters in E048653 and E048658 are compared in the first 100 ms of the discharges. Here, E048658 was tried after the similar plasma disruption with $W = 3.4$ MJ in the previous shot without any wall conditioning. In this series of the experimental plasmas, the plasma ramp-up was also assisted by ECH for break-down and heating in the initial phase. In E048653, and the plasma current smoothly ramped up with reduced ohmic electric field as low as 0.5 V/m. In E048658, the loop voltage was increased to the value that is limited by the power supply and this limit was not enough to induce the plasma current. At the beginning of the discharges just before the current ramp-up at $t = 105$ ms, a large difference in the particle recycling level was observed. In JT-60U, the particle recycling level has been measured with Hα/Dα photon emission detectors [10]. The neutral

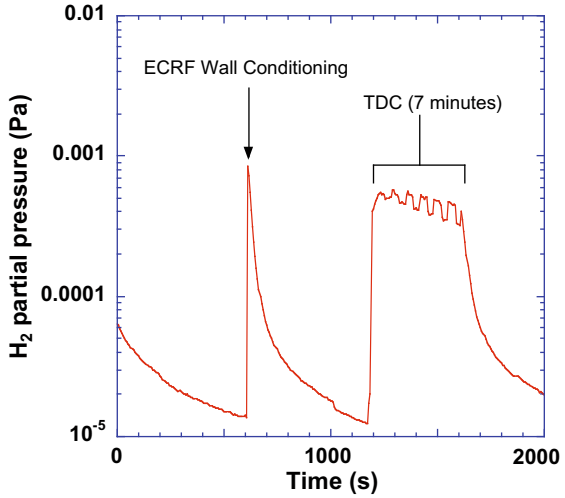

Fig. 3. H_2 outgas, measured by RGA, characteristics is compared between the ECH conditioning discharge and He TDC.

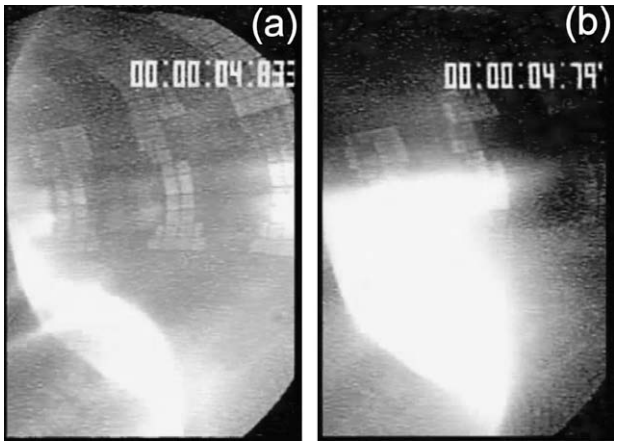

Fig. 4. Plasma images from CCD camera viewing inside the vacuum vessel. The center of torus is left. (a) Fundamental ECH ($B_T = 3.73$ T with $I_H = 4$ kA; (b) second harmonic ECH ($B_T = 1.86$ T) with $I_H = -4$ kA.

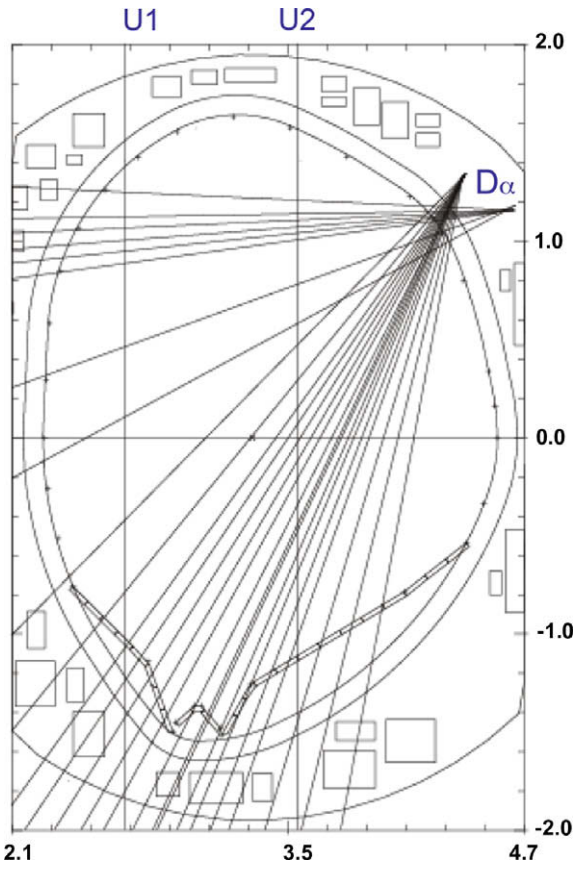

Fig. 5. Both the U1 and U2 chords for FIR laser interferometer are shown with Dα chords to measure the recycling level and the vacuum vessel.

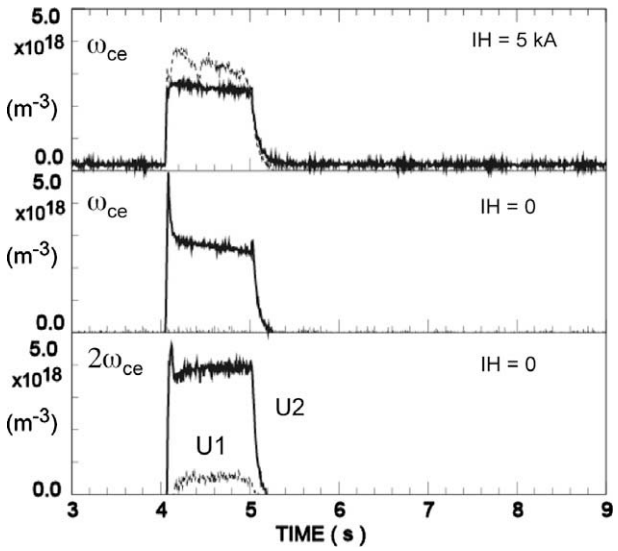

Fig. 6. Time traces of the U2 plasma density (thick solid lines) and the U1 plasma density (dashed line) when I_H is changed. The first and second column is for the fundamental ECH and the third column is for the second harmonic ECH.

ionization rate is calculated from the number of emitted Hα/Dα photons, using coefficients based upon those in Ref. [11], and the total recycling flux is determined by integrating the ionization density along the poloidal and toroidal circumferences.

Differences in these discharges are also shown in Fig. 8. In the first frame of the visible image after the plasma break-down, the much brighter hydrogen emissions was observed in E048658 along the resonant surface of ECH and on the inner baffle. In the second frame of E048658 at 33 ms later, hydrogen emission enhanced without the induction of the plasma current. This indicates that ECH power was not used to heat the main plasma in closed

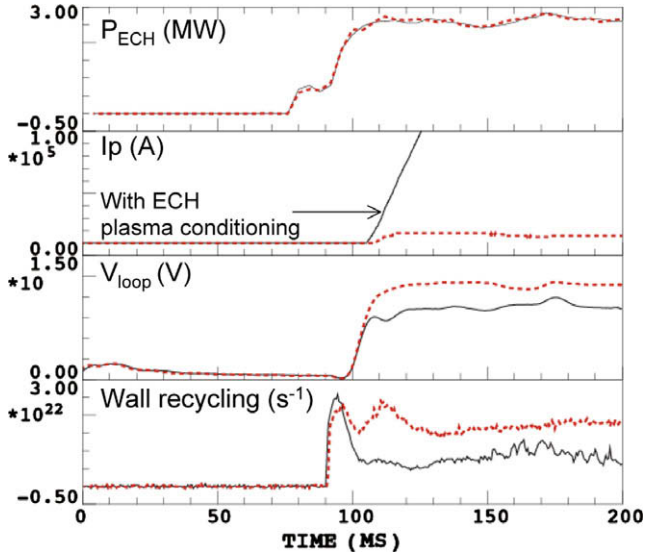

Fig. 7. Time traces of the plasma ramp-up, assisted by ECH, after the plasma disruptions at $W > 3$ MJ. Solid curves are with ECH plasma conditioning (E048653) and dotted curves are without any wall conditioning (E048658).

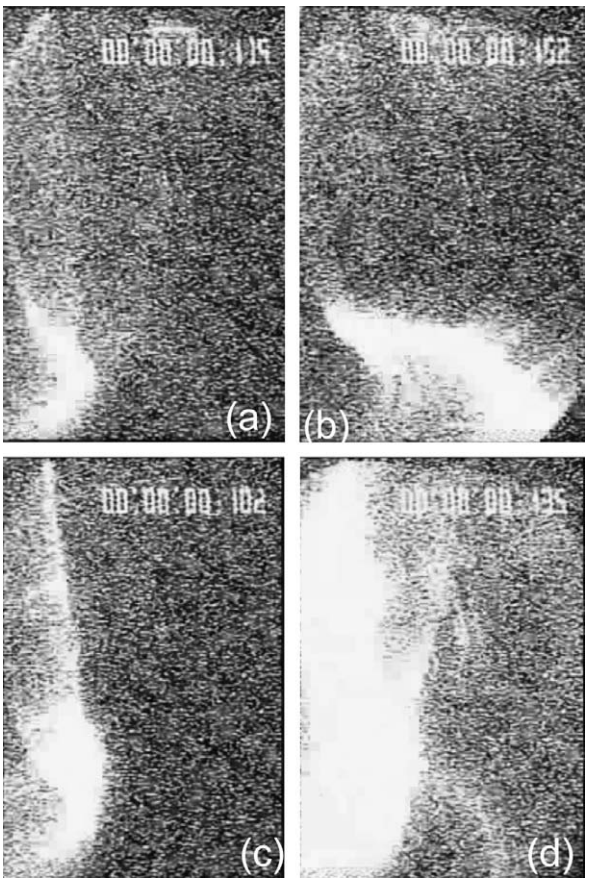

Fig. 8. Plasma images at the plasma start-up. The center of torus is left. (a) The first frame of E048653; (b) the second frame, 33 ms later; (c) the first frame of E048658 and (d) the second frame, 33 ms later.

magnetic surfaces to assist to ramp-up the plasma current. Instead, ECH power was used to ionize recycling hydrogen atoms. Once the loop voltage reached to the maximum value which corresponds to 0.5 V/m in E048658, there was no chance to ramp-up the plasma current to form closed magnetic surfaces.

In the second frame of the visible image in E048653, the plasma with closed flux surfaces expanded outward and it was limited by the outer baffle, because the recycling level was controlled by the wall conditioning discharge (E048652).

3. Summary and discussions

In series of experiments in 2000 and 2008, wall conditioning discharges under high $B_T = 3.6$ T were investigated by using the 110 GHz ECRF system of JT-60U.

Homogeneous He plasmas for wall conditioning were reproducibly obtained with the fundamental ECH when the horizontal field (0.5% of B_T strength) was applied in 2000. It was found that 2.4 Pa m^3 of He gas puff was optimum in terms of homogeneous plasma and the maximum H_2 outgas amount with $P_{ECRF} = 0.59$ MW and $t_{pulse} = 1$ s. With $P_{ECRF} = 1.27$ MW and $t_{pulse} = 1$ s, the efficiency of H_2 outgas in a minute was found to be as large as 79% of that in He TDC, which had been routinely used in JT-60U.

In 2008, additional experiment was carried out to investigate the horizontal field effect with reduced horizontal field (0.3% of B_T strength) and enhanced P_{ECRF}. It was found that the horizontal field is crucially important to expand He plasma toward the high field side from the fundamental ECH resonant surface.

The ECH wall conditioning discharge with $P_{ECRF} = 2.5$ MW and $t_{pulse} = 1.5$ s was applied after the plasma disruption with $W = 3.3$ MJ. The following experimental plasma was successfully started up with 0.5 V/m of ohmic electric field. While this start-up condition is slightly higher than that required for ITER, 0.3 V/m, ECH start-up with 0.26 V/m has been obtained with low ECH power, $P_{ECRF} = 0.4$ MW in JT-60U [12]. Therefore that the wall recovery by the ECH wall conditioning discharge is a promising technique for the fusion reactors. Further studies, including ECH power scan, will be necessary to improve accuracy for assessment of this technique for ITER and DEMO.

References

[1] J. Winter, J. Nucl. Mater. 161 (1989) 265.
[2] H.G. Esser et al., J. Nucl. Mater. 241–243 (1997) 861.
[3] E. Gauthier et al., J. Nucl. Mater 241–243 (1997) 553.
[4] J.S. Hu et al., J. Nucl. Mater. 376 (2008) 207.
[5] Y. Sakamoto et al., J. Nucl. Mater 93&94 (1980) 333.
[6] K. Ushigusa et al., Fus. Eng. Des. 45 (1999) 137.
[7] Y. Ikeda et al., Fus. Sci. Technol. 42 (2002) 435.
[8] N. Hosogane et al., J. Nucl. Mater. 220–222 (1995) 415.
[9] K.H. Finken et al., Rev. Sci. Instrum. 63 (1993) 1.
[10] N. Asakura et al., Nucl. Fus. 35 (1995) 381.
[11] L.C. Johnson, E. Hinov, J. Quant. Spectrosc. Radiat. Transf. 13 (1973) 333.
[12] K. Kajiwara et al., Nucl. Fus. 45 (2005) 694.